

Stiff polymer in monomer ensembleK. K. Müller-Nedebock,^{1,*} H. L. Frisch,^{1,2} and J. K. Percus^{3,4}¹*Department of Physics, University of Stellenbosch, Private Bag XI, Matieland, 7602 South Africa*²*Department of Chemistry, State University of New York at Albany, Albany, New York 12222*³*Courant Institute, New York University, New York 10012*⁴*Physics Department, New York University, New York 10012*

(Received 18 January 2002; revised manuscript received 14 October 2002; published 9 January 2003)

We employ an ordered monomer ensemble formalism in order to develop techniques to investigate a stiff polymer chain which is confined to a certain region. In particular, we calculate the segment density for a given location and segment orientation distribution within the confining geometry. With this method the role of the stiffness can be examined by means of differential equations, integral equations, or recursive relations for both continuum and lattice models. A suitable choice of lattice model permits an exact analytical solution for the segment location and orientation density for a chain between two parallel plates. For the stiff polymer in a spherical cavity we develop an integral equation formalism which is treated numerically, and in the same spherical geometry, a different model of the polymer displays a solution of a differential equation.

DOI: 10.1103/PhysRevE.67.011801

PACS number(s): 36.20.Ey, 82.35.Lr

I. INTRODUCTION

In this paper we develop and illustrate methods by which the segment orientation and density of polymer chains with stiffness and which are localized in a specified region of space may be computed. In two previous papers [1,2] a grand canonical partition function for noninteracting, flexible polymer chains was introduced in order to compute the chain segment density in the context of an ordered monomer ensemble. Here we introduce an angular dependence between polymer segments in this formalism. In particular, we illustrate computations relating to the stiffness of such a chain in constraining geometries. The effects of stiffness of polymers or their localization within pores or tubes frequently have been a topic of interest in polymer physics extending from biopolymers to liquid crystalline behavior as well as synthetic stiff and short polyamides [3–9]. Related work has been done by Ternovsky and co-workers [10] who developed a model of a stiff polymer near a wall in order to investigate adsorption of the chain to the surface. Stepanow [11], for example, has investigated a similar problem using the Kratky-Porod model for a semiflexible chain to write a differential equation for the end-to-end distance distribution. Ha and Thirumalai [13,12] have investigated stiff polymer chains under tension but without confining them to specific regions and Chirikjian and Wang [14] derived partial differential equations for the end-end orientation and location probability of a stiff polymer. However, work by Cordeiro, Molisana, and Thirumalai [15] has described conformational properties of flexible chains between plates. Furthermore, recent experimental work by Pfohl *et al.* [16] has investigated the orientation of biological macromolecules within microchannels.

In this paper we present the method and calculations for segment density of three different models of confined chains

with stiffness. These models all involve specific formulations of the stiffness and nature of the chains in the monomer ensemble. In one case analytic expressions for a polymer on a cubic lattice can be obtained. For chains in a continuum we show that torsional and flexural rigidities can be incorporated naturally by the monomer ensemble. In a spherical confining region it is possible to solve the associated integral equations numerically.

While we specifically show here how to compute segment densities of stiff *and confined* chains, it is worthwhile to note the underlying difficulties of some other mathematical treatments of the physics of wormlike polymers. For example, the well-known Kratky-Porod formulation for the wormlike chain introduces a bending energy term (with an associated constant τ) in a measure for the path $\mathbf{r}(s)$ of the chain, parametrized by the arc-length s ,

$$Z_{\text{KP}} = \int [d\mathbf{r}(s)] \exp\left(-\frac{1}{2\tau^2} \int_0^L ds \ddot{\mathbf{r}}^2(s)\right) \prod_s \delta(\dot{\mathbf{r}}^2(s) - 1) \times e^{-V/k_B T}. \quad (1.1)$$

V is an interaction term dependent on the nature of the problem under investigation. Although it is possible to calculate some properties of interest for this formalism analytically, there are many questions for which the constraint of unity of the tangential vector is extremely difficult to treat mathematically. In many cases, this condition can only be replaced by an average constraint of unity along the whole chain. Amongst many works, that of Gupta and Edwards [17] contains a discussion and several references. Wilhelm and Frey [4] also point out that the extreme limits for very flexible or extremely stiff chain limits are usually the only accessible ones in many calculations.

We use the previously introduced concepts [1,2]. By characterizing a bond position by a vector \mathbf{r} specifying its geometrical center and orientation, a bond fugacity $z(\mathbf{r})$

*Author to whom correspondence should be addressed. Email address: kkmn@physics.sun.ac.za

$=\langle \mathbf{r}|z|\mathbf{r}\rangle$ and interaction weight $w(\mathbf{r},\mathbf{r}')=\langle \mathbf{r}|w|\mathbf{r}'\rangle$, i.e., a Boltzmann factor, can be defined. The partition function for N bonds

$$\Xi_N = \int [d\mathbf{r}_1 d\mathbf{r}_2 \cdots d\mathbf{r}_N] \langle \mathbf{r}_1|z|\mathbf{r}_1\rangle \langle \mathbf{r}_1|w|\mathbf{r}_2\rangle \cdots \times \langle \mathbf{r}_{N-1}|w|\mathbf{r}_N\rangle \langle \mathbf{r}_N|z|\mathbf{r}_N\rangle. \quad (1.2)$$

This is used in order to write the expression for the grand canonical partition function as follows:

$$\Xi = 1 + \sum_{N=1}^{\infty} \langle \mathbf{1}|z(wz)^{N-1}|\mathbf{1}\rangle = 1 + \langle \mathbf{1}|z(I-wz)^{-1}|\mathbf{1}\rangle. \quad (1.3)$$

The vector $|\mathbf{1}\rangle$ is the vector of ones, resulting in the sum or integral over all spatial (and angular) locations. One can write for the number density

$$n(\mathbf{r}) = \frac{1}{\Xi} z(\mathbf{r}) \frac{\delta \Xi}{\delta z(\mathbf{r})}, \quad (1.4)$$

which gives

$$n(\mathbf{r}) = \frac{1}{\Xi} \langle \mathbf{1}|(I-zw)^{-1}|\mathbf{r}\rangle z(\mathbf{r}) \langle \mathbf{r}|(I-wz)^{-1}|\mathbf{1}\rangle. \quad (1.5)$$

By defining ψ and $\hat{\psi}$,

$$\psi(\mathbf{r}) = \langle \mathbf{r}|(I-wz)^{-1}|\mathbf{1}\rangle, \quad (1.6a)$$

$$\hat{\psi}(\mathbf{r}) = \langle \mathbf{1}|(I-zw)^{-1}|\mathbf{r}\rangle, \quad (1.6b)$$

one can simplify the expression for the density,

$$\frac{n(\mathbf{r})}{z(\mathbf{r})} = \frac{\psi(\mathbf{r})\hat{\psi}(\mathbf{r})}{\Xi}. \quad (1.7)$$

The grand canonical partition function is calculated from Eq. (1.3) as

$$\Xi = 1 + \int d\mathbf{r} z(\mathbf{r}) \psi(\mathbf{r}). \quad (1.8)$$

The average degree of polymerization is given by

$$\xi = \int d\mathbf{r} n(\mathbf{r}). \quad (1.9)$$

The solution of expressions (1.6a) and (1.6b) plays the central role in our calculations of the density.

Whereas in the previous works [1,2] the physical interpretation of the vector \mathbf{r} represented the location of the junction between any two segments of the polymer chains, the formalism is identical when a larger degree of freedom is represented by a vector of such a kind.

Therefore, in summary, we look at a sequence of segments described by their positions and orientations. These segments are linked into a chain by Boltzmann factors, w , for all consecutive pairs of segments. The chain ends are linked

to only one other segment. Furthermore, we associate to each segment a fugacity z which is dependent on the position and orientation of the given bond. The fugacity term can be used to represent an external potential acting on each segment, such as might be caused by confinement of the chain. The resulting partition function then leads to an expression for the segment density, which contains much useful information about the chain.

The expression for the chain segment density depends crucially on the quantities ψ and $\hat{\psi}$ which are defined in terms of w and z . We determine ψ and $\hat{\psi}$, and consequently $n(\mathbf{r})$, for three situations.

The bending energy terms for models of stiff chains could also be related to other quantities of interest for such chains such as the persistence length and end-to-end distance. Our method provides a direct means of calculating the local distribution of segments rather than correlations. The monomer ensemble, for example, permits relatively easy calculation for confined chains with which one cannot deal as readily in many other formulations which enable more direct computations of end-to-end distances. A more technical treatment (beyond the scope of this paper) within the monomer ensemble formalism could facilitate the determination of certain correlations.

The different approaches in this paper involve specific formulations of the stiffness which are incorporated into Eqs. (1.6a) and (1.6b) for the functions ψ in order to determine an expression for the density function (1.7). Section II shows the computation for the density of a discrete polymer confined between two parallel plates. In the Sec. III a general form for the integral equations for ψ of a chain with bending rigidity and torsion is derived. This method is illustrated by numerical results for the solution of the integral equations for a chain in a spherical container. Finally, a simple example for a differential equation formalism is presented in Sec. IV.

II. CONFINED POLYMER ON A CUBIC LATTICE

In this section we make use of a discrete formalism for stiff chains. In addition to associating a position on a cubic lattice, each segment also has one of six possible directions along the lattice. The bond direction is added to the previous bond position to give the next bond position for the chain. We map the states for the directions onto real-space unit vectors

$$\langle \sigma | \in \{ \langle 1 |, \dots, \langle 6 | \} \leftrightarrow \{ \hat{x}, \hat{y}, \hat{z}, -\hat{x}, -\hat{y}, -\hat{z} \} = \{ \hat{t}_\sigma \} \quad (2.1)$$

in a cartoon representation in which all bonds lie along coordinate axes and assign to each pair of bonds the weight

$$w(\mathbf{r}_1, \sigma_1; \mathbf{r}_2, \sigma_2) = \delta \left[\mathbf{r}_2 - \left(\mathbf{r}_1 + \frac{1}{2} \hat{t}_{\sigma_1} + \frac{1}{2} \hat{t}_{\sigma_2} \right) \right] \times \begin{cases} 1 & \text{if } \hat{t}_{\sigma_1} \cdot \hat{t}_{\sigma_2} = 1 \\ a & \text{if } \hat{t}_{\sigma_1} \cdot \hat{t}_{\sigma_2} = 0 \\ b & \text{if } \hat{t}_{\sigma_1} \cdot \hat{t}_{\sigma_2} = -1. \end{cases} \quad (2.2)$$

The first factor in the expression above constrains the centers of adjacent segments of the polymer; the second factor is responsible for the bending energetics. We express all lengths in terms of the step length of the walk. For the case when the chain is *free* transfer matrix techniques applied to the lattice model defined above can be used to determine the free energy and free chain persistence length. Indications of how this can be done are given in Appendix A.

Due to asymmetry under exchange of \mathbf{r}_1 and \mathbf{r}_2 of this interaction, two functions ψ , as defined earlier in Eqs. (1.6a) and (1.6b), are invoked

$$\hat{\psi}(\mathbf{r}, \sigma) = \langle \mathbf{1} | (I - zw)^{-1} | \mathbf{r}, \sigma \rangle \quad (2.3a)$$

$$\psi(\mathbf{r}, \sigma) = \langle \mathbf{r}, \sigma | (I - wz)^{-1} | \mathbf{1} \rangle, \quad (2.3b)$$

such that

$$1 = - \sum_{\sigma'} \int d^3 r' \langle \mathbf{r}, \sigma | w^T | \mathbf{r}', \sigma' \rangle z(\mathbf{r}', \sigma') \hat{\psi}(\mathbf{r}', \sigma') + \hat{\psi}(\mathbf{r}, \sigma), \quad (2.4a)$$

$$1 = - \sum_{\sigma'} \int d^3 r' \langle \mathbf{r}, \sigma | w | \mathbf{r}', \sigma' \rangle z(\mathbf{r}', \sigma') \psi(\mathbf{r}', \sigma') + \psi(\mathbf{r}, \sigma), \quad (2.4b)$$

where $d^3 r'$ is here a δ -function measure that converts integrals to sums over half-space lattices.

We investigate this polymer located between two parallel plates located at $r_z = \pm r_z^0 = \pm N$. At the plates the boundary conditions require that a segment of the polymer be oriented in parallel to the plate or perpendicularly away from it, but not perpendicularly into it:

$$z(r_z, \sigma) = \begin{cases} 0 & |r_z| > r_z^0 \\ 0 & r_z = r_z^0 \text{ and } \sigma = 3 \\ 0 & r_z = -r_z^0 \text{ and } \sigma = 6 \\ z_0 & \text{otherwise.} \end{cases} \quad (2.5)$$

Due to symmetry the functions ψ and $\hat{\psi}$ depend only on the z component of position and on σ . The x and y components are confined to a fixed large length and all thermodynamic potentials normalized appropriately. Furthermore, by comparing Eqs. (2.4a) and (2.4b) for ψ and $\hat{\psi}$ with the weight (2.2) substituted, we conclude that

$$\hat{\psi}(r_z, \sigma) = \psi(r_z, (\sigma + 3) \bmod 6), \quad (2.6)$$

with the convention that $\hat{\psi}(r_z, 6) = \hat{\psi}(r_z, 0)$. Under the above mentioned conditions we introduce the convenient notation

$$\psi(r_z, \sigma) = \begin{cases} \psi_{\parallel}(r_z) & \sigma = 1, 2, 4, 5 \\ \psi_{\uparrow}(r_z) & \sigma = 3 \\ \psi_{\downarrow}(r_z) & \sigma = 6. \end{cases} \quad (2.7)$$

Symmetry dictates that

$$\psi_{\parallel}(r_z) = \psi_{\parallel}(-r_z), \quad \text{and} \quad (2.8a)$$

$$\psi_{\uparrow}(r_z) = \psi_{\downarrow}(-r_z). \quad (2.8b)$$

Since ψ is defined in half lattice constants through weight (2.2), we shall also use the notation $\psi_{\uparrow}(r_z) = \psi_{\uparrow, m}$, where m is an integer or half integer, etc., interchangeably.

The following two Secs. II A and II B contain the information required to solve the Eqs. (2.4a) and (2.4b) for ψ and $\hat{\psi}$. The reader not interested in the procedure for solution may skip to Sec. II C.

A. System of equations

By inserting the bending energy and chain position, $-r_z^0 + 1 \leq r_z \leq r_z^0 - 1$, the factor w of Eq. (2.2) into the condition for ψ , Eq. (2.4b), the following equations are obtained after suitable translations:

$$1 = \psi_{\parallel}(r_z) [1 - z_0(1 + 2a + b)] - az_0 \psi_{\uparrow}\left(r_z + \frac{1}{2}\right) - az_0 \psi_{\downarrow}\left(r_z - \frac{1}{2}\right), \quad (2.9a)$$

$$1 = \psi_{\uparrow}\left(r_z - \frac{1}{2}\right) - bz_0 \psi_{\downarrow}\left(r_z - \frac{1}{2}\right) - z_0 \psi_{\uparrow}\left(r_z + \frac{1}{2}\right) - 4az_0 \psi_{\parallel}(r_z), \quad (2.9b)$$

$$1 = \psi_{\downarrow}\left(r_z + \frac{1}{2}\right) - bz_0 \psi_{\uparrow}\left(r_z + \frac{1}{2}\right) - z_0 \psi_{\downarrow}\left(r_z - \frac{1}{2}\right) - 4az_0 \psi_{\parallel}(r_z). \quad (2.9c)$$

These equations are valid away from the two plates acting as boundaries to the system. Consequently we shall refer to calculations relating to the above conditions as those pertaining to the ‘‘bulk.’’ By using the expressions from the above system [Eqs. (2.9a)–(2.9c)] $\psi_{\parallel}(r_z)$ can be eliminated, leaving equations expressing $\psi_{\uparrow}(r_z + 1/2)$ and $\psi_{\downarrow}(r_z + 1/2)$ in terms of $\psi_{\uparrow}(r_z - 1/2)$ and $\psi_{\downarrow}(r_z - 1/2)$. By defining the column vector

$$\boldsymbol{\psi}(r) = \begin{pmatrix} \psi_{\uparrow}(r) \\ \psi_{\downarrow}(r) \end{pmatrix}, \quad (2.10)$$

it is possible to relate functions of $\boldsymbol{\psi}$ at different steps by

$$\boldsymbol{\psi}(r + 1/2) = \mathbf{C} \cdot \boldsymbol{\psi}(r - 1/2) + \mathbf{D}, \quad (2.11)$$

with the matrices

$$\mathbf{C} = \begin{pmatrix} C_1 & C_2 \\ C_3 & C_4 \end{pmatrix}, \quad (2.12a)$$

$$\mathbf{D} = \begin{pmatrix} D_1 \\ -z_0(1 - b)D_1 \end{pmatrix}, \quad (2.12b)$$

with

$$C_1 = \frac{1 - z_0(1 + 2a + b)}{z_0[1 - z_0(1 + 2a + b) + 4a^2z_0]} \quad (2.12c)$$

$$= \frac{(1 + C_2)}{z_0(1 - b)}, \quad (2.12d)$$

$$C_2 = -\frac{b[1 - z_0(1 + 2a + b)] + 4a^2z_0}{[1 - z_0(1 + 2a + b) + 4a^2z_0]} \quad (2.12e)$$

$$C_3 = -C_2, \quad (2.12f)$$

$$C_4 = z_0(1 - b)(1 - C_2), \quad (2.12g)$$

$$D_1 = -\frac{1 - z_0(1 + 2a + b) + 4az_0}{z_0[1 - z_0(1 + 2a + b) + 4a^2z_0]}. \quad (2.12h)$$

As a consequence any ‘‘bulk’’ values of ψ can be calculated given the values of ψ at a point (integer and half-integer) on the lattice:

$$\psi_{n+m} = C^n \psi_m + (C-1)^{-1}(C^n - 1)D, \quad (2.13a)$$

$$\psi_{n+m+1/2} = C^n \psi_{m+1/2} + (C-1)^{-1}(C^n - 1)D. \quad (2.13b)$$

Before commencing on further calculations we note:

(i) According to Eq. (2.9a) $\psi_{\parallel}(r)$ can be computed with the knowledge of $\psi(r \pm 1/2)$.

(ii) The matrix C can be written in terms of C_2 as follows:

$$C = \begin{pmatrix} \frac{1 + C_2}{z_0(1 - b)} & C_2 \\ -C_2 & z_0(1 - b)(1 - C_2) \end{pmatrix}. \quad (2.14)$$

A simple calculation shows that the determinant of the matrix is 1, which means that its two eigenvalues are inverses of one another.

B. Boundary conditions and solution

To determine values of ψ it is necessary to use Eqs. (2.13a) and (2.13b) in conjunction with the conditions at the plates confining the polymer. When $r_z \geq N - \frac{1}{2}$ it is necessary to refer to the full equations for ψ (2.4b) rather than the bulk values used in the preceding subsection. Equations at the upper plate, for example, are readily derived and recorded in Appendix C.

Equations (C4b) and (C5) relate $\psi_{\uparrow N-1}$ to $\psi_{\downarrow N-1}$ and Eqs. (C3c) and (C4a) relate $\psi_{\uparrow N-1/2}$ to $\psi_{\downarrow N-1/2}$.

$$1 = -\frac{4az_0}{1 - z_0(1 + 2a + b)} + \psi_{\uparrow, N-1} - \left(\frac{4a^2z_0^2}{1 - z_0(1 + 2a + b)} + bz_0 \right) \psi_{\downarrow, N-1}, \quad (2.15a)$$

$$1 = -\frac{4az_0}{1 - z_0(1 + 2a + b)} + \psi_{\uparrow, N-1/2} - \left(\frac{4a^2z_0^2}{1 - z_0(1 + 2a + b)} + bz_0 \right) \psi_{\downarrow, N-1/2}. \quad (2.15b)$$

Similarly, one can derive for the bottom plate,

$$1 = -\frac{4az_0}{1 - z_0(1 + 2a + b)} + \psi_{\downarrow, -N+1} - \left(\frac{4a^2z_0^2}{1 - z_0(1 + 2a + b)} + bz_0 \right) \psi_{\uparrow, -N+1}, \quad (2.15c)$$

$$1 = -\frac{4az_0}{1 - z_0(1 + 2a + b)} + \psi_{\downarrow, -N+1/2} - \left(\frac{4a^2z_0^2}{1 - z_0(1 + 2a + b)} + bz_0 \right) \psi_{\uparrow, -N+1/2}. \quad (2.15d)$$

A solvable system of equations now remains. We know from the boundary conditions given above that the two component of the column vector ψ_{N-1} are not independent and we also know from Eq. (2.13a) that ψ_{N-1} is related to ψ_{-N+1} . All remaining values for the function ψ can be determined from the expressions in Appendix C and from the results of the preceding subsection.

The relationship between ψ_{N-1} and ψ_{-N+1} is

$$\psi_{N-1} = C^{2N-2} \psi_{-N+1} + (C-1)^{-1}(C^{2N-2} - 1)D. \quad (2.16)$$

Together with the boundary conditions (2.15a) and (2.15b), it is straightforward to determine the value of ψ_{N-1} from which all other values of ψ can be calculated.

The left and right matrices, L and R , of C diagonalize C ,

$$LCR = \begin{pmatrix} \lambda_+ & 0 \\ 0 & \lambda_- \end{pmatrix} \equiv \begin{pmatrix} \lambda & 0 \\ 0 & \lambda^{-1} \end{pmatrix}, \quad (2.17)$$

$$\text{where } LR = RL = 1, \quad (2.18)$$

$$\text{with } L \equiv \begin{pmatrix} L_1 & L_2 \\ L_3 & L_4 \end{pmatrix}, \quad (2.19)$$

$$\text{and } \lambda_{\pm} = \frac{1}{2} \left[z_0(1 - b)(1 - C_2) + \frac{1 + C_2}{z_0(1 - b)} \right] \pm \frac{1}{2} \sqrt{\left(z_0(1 - b)(1 - C_2) + \frac{1 + C_2}{z_0(1 - b)} \right)^2 - 4}. \quad (2.20)$$

Equation (2.16) becomes

$$\mathbf{L}\psi_{N-1} = \begin{pmatrix} \lambda_+^{2N-2} & 0 \\ 0 & \lambda_-^{2N-2} \end{pmatrix} \mathbf{L}\psi_{-N+1} + \begin{pmatrix} \frac{\lambda_+^{2N-2}-1}{\lambda_+-1} & 0 \\ 0 & \frac{\lambda_-^{2N-2}-1}{\lambda_- -1} \end{pmatrix} \mathbf{L}\mathbf{D}. \quad (2.21)$$

The solution is

$$\begin{aligned} \psi_{\downarrow, N-1} = & \left\{ \left[L_3 X_1 - \lambda^{-2N+2} L_4 X_1 - \frac{\lambda^{-2N+2}-1}{\lambda^{-1}-1} (L_3 D_1 \right. \right. \\ & \left. \left. + L_4 D_2) \right] (\lambda^{-2N+2} L_3 + \lambda^{-2N+2} L_4 X_3)^{-1} \right. \\ & \times (\lambda^{2N-2} L_1 + \lambda^{2N-2} L_2 X_2) + \left[\lambda^{2N-2} L_2 X_1 - L_1 X_1 \right. \\ & \left. + \frac{\lambda^{2N-2}-1}{\lambda-1} (L_1 D_1 + L_2 D_2) \right] \Bigg\} / \{ L_1 X_2 + L_2 \\ & - \lambda^{4N-4} (L_1 + L_2 X_2) (L_3 + L_4 X_2)^{-1} (L_3 X_2 + L_4) \}, \end{aligned} \quad (2.22)$$

where we have defined

$$X_1 = 1 + \frac{4az_0}{1-z_0(1+2a+b)}, \quad \text{and} \quad (2.23)$$

$$X_2 = \frac{4a^2 z_0^2}{1-z_0(1+2a+b)} + bz_0. \quad (2.24)$$

(They are the constant and coefficient in the boundary condition equations.) Standard methods can be used to find complete (albeit lengthy) expressions for L_1, \dots, L_4 .

Clearly, solution (2.22) is lengthy to write out in full, although it is given explicitly. It is simpler to consider limiting expressions. For the purposes of this we shall choose a specific case, where $b=a^2$ and $0 < a < 1$, and expand to first order in $\epsilon = a$, i.e., the case of an extremely stiff polymer. Functions for this scenario are labeled by a superscript ‘‘S.’’

For the stiff case and for $n \in \mathbb{Z}^+$ we have,

$$\mathbf{C}^n \simeq \begin{pmatrix} z_0^{-n} & 0 \\ 0 & z_0^n \end{pmatrix} + O(\epsilon^2), \quad (2.25)$$

$$\begin{aligned} \mathbf{E}_n \simeq & \begin{pmatrix} \frac{z_0}{1-z_0} (z_0^{-n}-1) & 0 \\ 0 & \frac{1}{z_0-1} (z_0^n-1) \end{pmatrix} \\ & \times \begin{pmatrix} -\frac{1}{z_0} - \frac{4}{1-z_0} \epsilon \\ 1 + \frac{4z_0}{1-z_0} \epsilon \end{pmatrix} + O(\epsilon^2), \end{aligned} \quad (2.26)$$

$$\text{where } \mathbf{E}_n \equiv (\mathbf{C}-1)^{-1} (\mathbf{C}^n - 1) \mathbf{D}. \quad (2.27)$$

$$\begin{aligned} \psi_{\downarrow, N-1}^S = & \psi_{\uparrow, -N+1}^S \simeq z_0^{2N-2} + \frac{1}{z_0-1} (z_0^{2N-2}-1) + \epsilon \left(\frac{4z_0}{1-z_0} \right) \\ & \times \left[z_0^{2N-2} + \frac{z_0^{2N-2}-1}{z_0-1} \right], \end{aligned} \quad (2.28)$$

$$\begin{aligned} \psi_{\downarrow, 0}^S = & \psi_{\uparrow, 0}^S \simeq z_0^{N-1} \left(1 - \frac{1}{1-z_0} \right) + \frac{1}{1-z_0} + \epsilon \frac{4z_0}{1-z_0} \left[\frac{1}{1-z_0} \right. \\ & \left. + z_0^{N-1} \left(1 - \frac{1}{1-z_0} \right) \right], \end{aligned} \quad (2.29)$$

$$\psi_{\parallel, 0}^S = \frac{1}{1-z_0} + \epsilon \frac{2z_0}{1-z_0} \left[\frac{1}{1-z_0} + z_0^{N-1} + \frac{1}{1-z_0} (1-z_0^{N-1}) \right]. \quad (2.30)$$

Similarly we have the following approximation for the floppy (‘‘F’’) case, where $a=b=1$,

$$\mathbf{C}^F = \begin{pmatrix} \frac{1-4z_0}{z_0} & -1 \\ 1 & 0 \end{pmatrix}. \quad (2.31)$$

C. The grand canonical partition function, the density, and average degree of polymerization

The grand canonical partition function, which also features in the expression for the density (1.7), for the discrete model is given as usual by

$$\begin{aligned} \Xi &= 1 + \sum_{\sigma} \sum_{\{r\}} z(r, \sigma) \psi(r, \sigma) \\ &= 1 + 2z_0 (4\psi_{\parallel, -N} + \psi_{\uparrow, -N}) + z_0 (1, 1) \cdot (1-\mathbf{C})^{-1} \\ & \quad \times \{ (1-\mathbf{C}^{2N}) \psi_{-N+1/2} + (1-\mathbf{C}^{2N-1}) \psi_{-N+1} \\ & \quad + [(1-\mathbf{C})^{-1} (1-\mathbf{C}^{2N}) - 2N\mathbf{1}] \cdot \mathbf{D} + [(1-\mathbf{C})^{-1} \\ & \quad \times (1-\mathbf{C}^{2N-1}) - (2N-1)\mathbf{1}] \cdot \mathbf{D} \}. \end{aligned} \quad (2.32)$$

It is a number dependent on N, z_0, a , and b .

The parameters of the present model can be understood to give two different types of behavior when considering, for example, the parallel and perpendicular orientations at the center of the two plates. We wish to investigate the ratio of the probability that the segments in the middle of the plates have a perpendicular orientation with respect to the plates to the probability that they are parallel to the plates using Eq. (1.7),

$$\frac{n(0, \uparrow)}{n(0, \parallel)} = \frac{\psi_0^2}{\psi_{\parallel}^2(0)}. \quad (2.33)$$

The values of $\psi_{\uparrow}(0)$ and $\psi_{\parallel}(0)$ at the center are easily calculated according to the scheme in Appendix C and in preceding sections of the paper.

We calculate the ratio $n(0,\uparrow)/n(0,\parallel)$ for the limiting case where a and $b \equiv a^2$ are almost equal to 0 using Eqs. (2.29) and (2.30) (the ‘‘stiff’’ case labeled by ‘‘S’’).

$$\frac{n^S(0,\uparrow)}{n^S(0,\parallel)} \approx \frac{z_0^{N-1} \left(1 - \frac{1}{1-z_0} \right) + \frac{1}{1-z_0} + \epsilon \frac{4z_0}{1-z_0} \left[\frac{1}{1-z_0} + z_0^{N-1} \left(1 - \frac{1}{1-z_0} \right) \right]}{\frac{1}{1-z_0} + \epsilon \frac{2z_0}{1-z_0} \left[\frac{1}{1-z_0} + z_0^{N-1} + \frac{1}{1-z_0} (1-z_0^{N-1}) \right]}. \quad (2.34)$$

For chains with a low fugacity and plates which are far apart, this ratio approaches 1, indicating that the chain segments are isotropic in the center. For the stiff case it can be seen clearly that for long chains and small plate spacing most of the polymer is parallel to the plates.

The degree of polymerization (1.9) can also be evaluated

$$\xi = \frac{2z_0}{\Xi} \left\{ [\psi_0^2 + 2\psi_{\parallel}^2] + 2 \sum_{i=1}^N (\psi_{\uparrow,i} \psi_{\downarrow,i} + 2\psi_{\parallel,i}^2) \right\}. \quad (2.35)$$

The summation above also contains the nonbulk contributions at the edges of the system.

In theory it is also possible to compute averages of end-to-end distances for confined polymers using the monomer ensemble method. This would require alterations to the fugacity term and calculations beyond the scope of this paper and is briefly discussed in Appendix B.

The Potts-type model which has been discussed in the present section can also be investigated from the viewpoint of a set of differential equations. The discrete ‘‘bulk equations’’ can be converted into differential equations by expanding around r_z to second order. The coupled set of differential equations can be solved by Laplace transformation. The need to solve for the roots of a fourth-order polynomial for the inverse Laplace transform means that this method does not bring about much of a simplification of the system.

III. INTEGRAL EQUATION

To obtain an integral equation for a system with stiffness one can employ a system of double labeling of successive bonds. Thus one can write for the partition function

$$\Xi_N = \int da da' db db' \cdots \langle a|w|a' \rangle \langle a'|z|b \rangle \langle b|w|b' \rangle \cdots, \quad (3.1)$$

where the a, a', b, b', \dots denote successive bonds. The scheme is illustrated in Fig. 1. For the bond labeled either 3 or 2' in Fig. 1 the unit vector for the bend can be computed by means of $(\mathbf{r}_2 - \mathbf{r}_3)$ and $(\mathbf{r}_3 - \mathbf{r}_4)$. The torsional angle can be computed by taking more vectors into account and can be constructed by investigating, for example, $(\mathbf{r}_1 - \mathbf{r}_2) \times (\mathbf{r}_2 - \mathbf{r}_3)$ in relation to $(\mathbf{r}_3 - \mathbf{r}_4) \times (\mathbf{r}_4 - \mathbf{r}_5)$. The full torsional and bending energy at position 3 in Fig. 1 is then expressed through a potential $V(\mathbf{r}_1, \mathbf{r}_2, \mathbf{r}_3, \mathbf{r}_4, \mathbf{r}_5) = V(\vec{\mathbf{r}}_3)$ which can be written as a weight in the chemical potential factor z

$= z(\vec{\mathbf{r}}_3) = \exp[-\beta V(\vec{\mathbf{r}}_3)]$, with $\vec{\mathbf{r}}_3$ representing the supervector centered around position 3. The role of w lies in connecting the other points correctly for the preceding and succeeding bond-related angles. It does this as follows:

$$\begin{aligned} & \cdots \langle \vec{\mathbf{r}}|z|\vec{\mathbf{r}} \rangle \langle \vec{\mathbf{r}}|w|\vec{\mathbf{r}}' \rangle \langle \vec{\mathbf{r}}'|z|\vec{\mathbf{r}}' \rangle \cdots \\ & = \cdots \langle \vec{\mathbf{r}}|z|\vec{\mathbf{r}} \rangle \delta(\mathbf{r}'_1 - \mathbf{r}_2) \delta(\mathbf{r}'_2 - \mathbf{r}_3) \delta(\mathbf{r}'_3 - \mathbf{r}_4) \delta(\mathbf{r}'_4 - \mathbf{r}_5) \\ & \quad \times \langle \vec{\mathbf{r}}'|z|\vec{\mathbf{r}}' \rangle \cdots \end{aligned}$$

Part (b) of Fig. 1 shows how the preceding mathematical prescription of labeling follows when the monomers are viewed as having internal structure, with appropriate weights for internal conformations. The monomers interact so that appropriate parts of the substructure coincide. This fixes z and w , respectively. We remark that there are several possi-

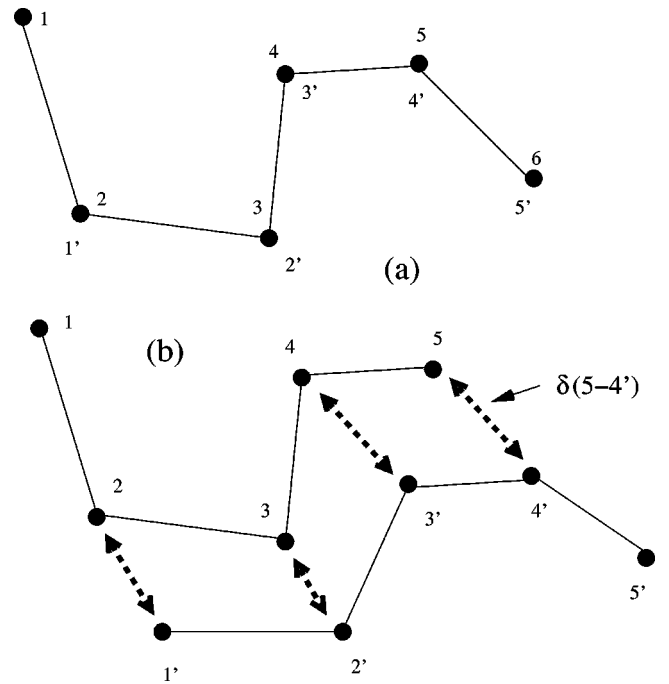


FIG. 1. The figure depicts the double labeling scheme in part (a). This scheme can also be seen to emerge from δ -function Boltzmann factors connecting monomers with five-segment structures, as depicted in part (b) of the figure. The dashed double arrows indicate which parts of the monomer 12345 must be the same physical locations on the monomer 1'2'3'4'5'. In this way the dashed double arrows are δ functions of the respective positions. We show one such δ function joining points 5 and 4'.

bilities to incorporate flexural and bending terms in the integral equation formalism; we shall illustrate one such way.

The equation for $\psi(\vec{r})$ becomes

$$\psi(\vec{r}) = \langle \vec{r} | (I - wz)^{-1} | \mathbf{1} \rangle, \quad (3.2)$$

leading to

$$1 = \psi(\mathbf{r}_1 \mathbf{r}_2 \mathbf{r}_3 \mathbf{r}_4 \mathbf{r}_5) - \int d^3 r'_5 z(\mathbf{r}_2 \mathbf{r}_3 \mathbf{r}_4 \mathbf{r}_5 \mathbf{r}'_5) \psi(\mathbf{r}_2 \mathbf{r}_3 \mathbf{r}_4 \mathbf{r}_5 \mathbf{r}'_5). \quad (3.3)$$

By assuming simple bending without torsional effects, the description can be simplified by making use of three consecutive position coordinates:

$$\psi(\mathbf{r}_1 \mathbf{r}_2 \mathbf{r}_3) = 1 + \int d^3 r' z(\mathbf{r}_2 \mathbf{r}_3 \mathbf{r}') \psi(\mathbf{r}_2 \mathbf{r}_3 \mathbf{r}'), \quad (3.4a)$$

and

$$\hat{\psi}(\mathbf{r}_1 \mathbf{r}_2 \mathbf{r}_3) = 1 + \int d^3 r' z(\mathbf{r}' \mathbf{r}_1 \mathbf{r}_2) \hat{\psi}(\mathbf{r}' \mathbf{r}_1 \mathbf{r}_2). \quad (3.4b)$$

A model that lends itself readily to an iterative numerical solution is that of the chain of segments of fixed length which is confined to a spherical region. A bending probability for two adjacent segments labeled 12 and 23, with unit vectors \hat{n}_{12} and \hat{n}_{23} , can be assigned

$$P(\hat{n}_{12}, \hat{n}_{23}) = p(1 + \hat{n}_{12} \cdot \hat{n}_{23}). \quad (3.5)$$

This causes the forward direction to be favored, with $p > 0$. The function of $z = z(\mathbf{r}_1, \mathbf{r}_2, \mathbf{r}_3)$ in this model is to restrict $\mathbf{r}_1 - \mathbf{r}_2 = \hat{n}_{12}$ and $\mathbf{r}_2 - \mathbf{r}_3 = \hat{n}_{23}$ to unit vectors, and to keep the vectors for the spatial locations of bonds $\mathbf{r}_1, \mathbf{r}_2$, and \mathbf{r}_3 from going out of the confines of the sphere. Consequently, one can write

$$z(\mathbf{r}_1, \mathbf{r}_2, \mathbf{r}_3) = p(1 + \hat{n}_{12} \cdot \hat{n}_{23}) \delta(|\hat{n}_{12}| - 1) \delta(|\hat{n}_{23}| - 1) \times \vartheta(R - |\mathbf{r}_1|) \vartheta(R - |\mathbf{r}_2|) \vartheta(R - |\mathbf{r}_3|), \quad (3.6)$$

where R is the radius of the confining sphere and ϑ is the Heavyside step function.

The spherical symmetry and Eqs. (3.6) and (3.4a) require the following dependence:

$$\psi(\mathbf{r}_1 \mathbf{r}_2 \mathbf{r}_3) = \psi(|\mathbf{r}_2|, n_{23,r}), \quad (3.7)$$

where $n_{23,r}$ is the radial component of the unit vector \hat{n}_{23} .

A. Results

In a numerical scheme to solve the equations, it is possible to iterate equation (3.4a) at different values of the parameters. By rewriting the basic integral equation with P , given by Eq. (3.5), one has

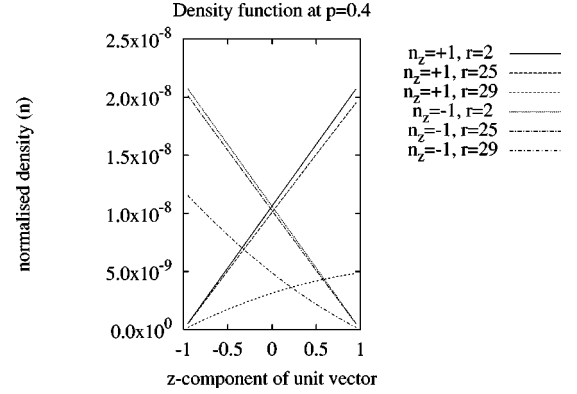


FIG. 2. Plot of the density at different radii for $R=30$ and $p=0.4$. Dependence on the radial component of the first of the two consecutive vectors is shown, with the different lines representing the second segment oriented either outward or inward along the radius at different positions within the sphere. Right- and left-sloping lines represent forward and backward directions, respectively. We see how the straight conformation is much favored for regions with small r well inside the sphere. Near the boundary (at $r=30$) the straight outward orientation (both unit vector components equal to $+1$) is seen to be greatly suppressed.

$$\psi(\mathbf{r}, n_r) = 1 + \int d\hat{n}' p(1 + \hat{n} \cdot \hat{n}') \tilde{z} \psi(\mathbf{r} + \hat{n}, \hat{n}'). \quad (3.8)$$

In this equation \tilde{z} ensures that the positions of the bonds remain within the spherical region. We find (Appendix D) that ψ can be split into a sum of two parts in successive spherical shells, one of which is only a function of the radial distance r and another which is directly proportional to the radial component of the unit vector n_r , multiplied by a function of r only. Therefore, to integrate from one spherical shell to the next we write:

$$\psi(\mathbf{r}, n_r) \equiv \phi_1(r) + n_r \phi_2(r). \quad (3.9)$$

With this manner of splitting the function ψ it is possible to divide the system into a number of spherical shells for each of which a ϕ_1 and ϕ_2 have been defined. Equation (3.8) for ψ can be iterated until the values converge. The integration scheme for the different shells is discussed in Appendix D.

With the knowledge of ψ the value of Ξ can be computed, and the density expression is

$$n(\hat{n}_{12}, |\mathbf{r}_2|, \hat{n}_{23}) = \frac{1}{\Xi} p(1 + \hat{n}_{12} \cdot \hat{n}_{23}) \psi(r_2, n_{12,r}) \psi(r_2, n_{23,r}). \quad (3.10)$$

This five-dimensional quantity can be plotted in a variety of manners. In Fig. 2 we plot the density at three different radii in dependence on the r component of \hat{n}_{23} and both unit vectors lying in the same plane. The other directional component is chosen as lying either radially outward $n_z = +1$ or radially inward $n_z = -1$. For central regions of the sphere we see that the straight configuration is favored and that the angular distribution is more-or-less isotropic, i.e., that both unit vectors lying inwards pointing or outwards pointing is almost

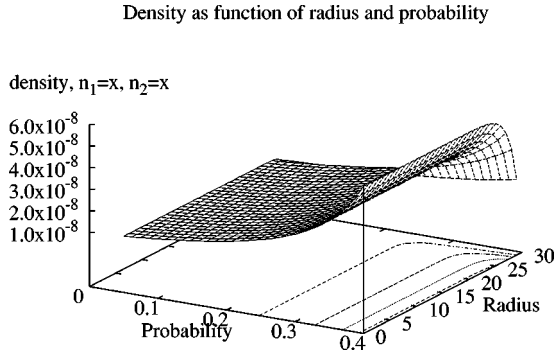


FIG. 3. Plot of the density at different radii for $R = 30$ and various values of p . The significant decrease of the probability of the straight orientation near the boundary can be seen clearly.

equally probable. This changes appreciably at the sides, where the radially outward density is considerably lower than the inwards-facing case.

In Fig. 3 the density for both unit vectors perpendicular to the radial direction and the bond being straight is plotted as a function of the radius and the probability p . The density decreases towards the boundary of the system, located at $R = 30$, and increases with p . Note that the chemical potential is built in through p .

From these graphs a clear picture emerges of a chain which is homogeneous in the center of the confining sphere and which becomes depleted at the boundaries. At these boundaries a tangential orientation of the segments is considerably favored above the perpendicular (radial) case.

In Fig. 4 the dependence of the degree of polymerization on the combined probability and chemical potential p is shown.

B. Possible alternative methods for solution

Another method to solve the integral equation is making use of an expansion in terms of eigenfunctions, and using successive substitutions to determine coefficients. For the case of Eq. (3.4a) a weight

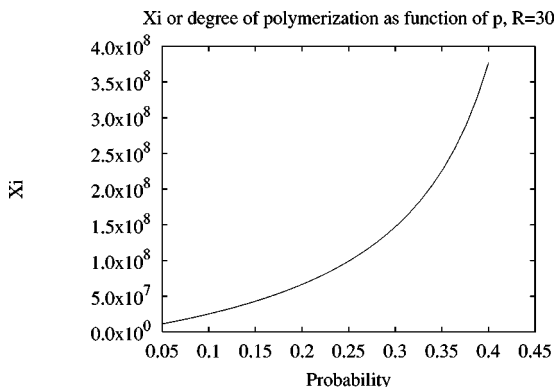


FIG. 4. Plot of the degree of polymerization at a function of p .

$$z(\mathbf{r}_1\mathbf{r}_2\mathbf{r}_3) = \mathcal{N} \bar{\vartheta} [(\mathbf{r}_2 - \mathbf{r}_1) \cdot (\mathbf{r}_3 - \mathbf{r}_2)]^2 \\ \times (\mathbf{r}_2 - \mathbf{r}_1)^2 \exp\left(-\frac{1}{\ell^2}(\mathbf{r}_2 - \mathbf{r}_1)^2\right) \\ \times (\mathbf{r}_3 - \mathbf{r}_2)^2 \exp\left(-\frac{1}{\ell^2}(\mathbf{r}_3 - \mathbf{r}_2)^2\right) \quad (3.11)$$

could be introduced. The first factor after $\bar{\vartheta}$ [which, as in Eq. (3.6), confines points to an appropriate region] represents the bending interaction term of the type $\cos^2\theta$ between two bonds, while the peaked functions $x^2 \exp(-x^2)$ set a length scale to the segments. \mathcal{N} is a normalization.

The weight z and ψ can be expressed as a sum of (generalized) Hermite polynomials [18]

$$z(\mathbf{r}_1\mathbf{r}_2\mathbf{r}_3) = \sum_n q_n \langle H_n | \mathbf{r}_1\mathbf{r}_2\mathbf{r}_3 \rangle, \quad (3.12)$$

$$\psi(\mathbf{r}_1\mathbf{r}_2\mathbf{r}_3) = \sum_m y_m \langle \mathbf{r}_1\mathbf{r}_2\mathbf{r}_3 | H_m \rangle. \quad (3.13)$$

These functions could be inserted into bending integral equation (3.4a), and terms compared.

IV. DIFFERENTIAL EQUATION FORM

In Ref. [1] the density distribution for a polymer confined to a spherical cavity was computed by expressing ψ in Eq. (1.6a) as

$$z\psi = w^{-1}(\psi - 1), \quad (4.1)$$

and by making the appropriate choices for the fugacity inside and outside the cavity. The inverse Boltzmann factor w^{-1} was taken to be the differential operator of which w is the Green function. A suitable choice was that of a Yukawa form leading to a Helmholtz operator,

$$\delta(\mathbf{r} - \mathbf{r}') = w^{-1} \frac{A e^{-K|\mathbf{r} - \mathbf{r}'|}}{|\mathbf{r} - \mathbf{r}'|} = \frac{-1}{4\pi A} (\nabla^2 - K^2) w. \quad (4.2)$$

A solution can be found readily for this system.

In order to introduce stiffness a segment of the polymer chain is now described by the positions of its ends \mathbf{x}, \mathbf{x}' and the orientation of those ends \hat{n}, \hat{n}' . Clearly, for a rod ($\mathbf{x} - \mathbf{x}'$), \hat{n} and \hat{n}' are related. The vector $|\mathbf{r}\rangle$ then has the dependence $|\mathbf{r}\rangle = |\mathbf{x}, \vartheta, \phi\rangle$. By noting that,

$$\left(\frac{-1}{a^2}\right) \left(\frac{\partial^2}{\partial \alpha^2} - a^2\right) \left[\frac{a}{2} e^{-a|\alpha - \alpha'|}\right] = \delta(\alpha - \alpha'), \quad (4.3)$$

a simple multiplicative, bending ‘‘Boltzmann’’ factor is introduced,

$$w(\mathbf{x}, \vartheta, \phi; \mathbf{x}', \vartheta', \phi') = \frac{Aab}{4|x-x'|} e^{-a|\vartheta-\vartheta'|-b|\phi-\phi'|-K|x-x'|}. \quad (4.4)$$

The substitution

$$\psi - 1 = \frac{\eta(\mathbf{r})}{|\mathbf{r}|} \xi(\vartheta) \zeta(\phi) \quad (4.5)$$

will separate the variables. For the spherical container we need to solve

$$\left(\frac{\partial^2}{\partial \vartheta^2} - a^2 \right) \left(\frac{\partial^2}{\partial \phi^2} - b^2 \right) (\nabla^2 - K^2) \eta(x) \xi(\vartheta) \zeta(\phi) = 0, \quad (4.6)$$

for the outside and

$$z_0 = \left(\frac{\partial^2}{\partial \vartheta^2} - a^2 \right) \left(\frac{\partial^2}{\partial \phi^2} - b^2 \right) (\nabla^2 - K^2) \frac{\eta}{x} \xi \zeta + 4\pi a^2 b^2 z_0 \frac{\eta}{x} \xi \zeta, \quad (4.7)$$

for the inside. For the outside the usual radial solution is obtained, whereas for the inside of the sphere we have

$$\left(\frac{\partial^2}{\partial \vartheta^2} - a^2 \right) \xi = c_\xi \xi, \quad (4.8)$$

$$\left(\frac{\partial^2}{\partial \phi^2} - b^2 \right) \zeta = c_\zeta \zeta, \quad (4.9)$$

$$\left(\frac{\partial^2}{\partial x^2} - K^2 \right) \eta = c_\eta \eta, \quad (4.10)$$

where

$$c_\xi c_\zeta c_\eta = -4\pi A a^2 b^2. \quad (4.11)$$

Here the radial distance and orientation of parts of the chain are completely decoupled. This is physically acceptable. We impose the fact that the boundary conditions are cyclic in that $\xi(\vartheta + 2\pi) = \xi(\vartheta)$ and $\zeta(\phi + \pi) = \zeta(\phi)$. For the polymer confined to the spherical cavity, the external solution for r only is required. The results for r are identical to the results in [1]

$$r(\psi(r) - 1) = \frac{K^2 - K'^2}{K'^2} \left(r - \frac{(1 + KR) \sinh K' r}{K \sinh K' R + K' \cosh K' R} \right), \quad r \leq R. \quad (4.12)$$

Since the solutions to Eqs. (4.8) and (4.9) have to be periodic or constant, the condition on the constants c_ξ and c_ζ are that

$$c_\xi + a^2 \leq 0 \quad \text{and} \quad (4.13)$$

$$c_\zeta + b^2 \leq 0. \quad (4.14)$$

With Eq. (4.11), c_η must be negative.

V. CONCLUSIONS

In summary, the formalism we have presented lends itself for tackling the difficult problem of a chain which is both stiff *and* confined. Although it is possible, in principle, in our method (see Appendix B), we do not calculate end-to-end vector averages, but can express the distributions of the orientation and location of polymer chain segments. In our formalism it is relatively simple to implement constraints and chain stiffness. Its strength lies in this simplicity and powerfulness with respect to the usually tedious route of implementing, for example, the wormlike chain constraints of the Kratky-Porod model when computing statistical physical averages. In many of the alternative approaches the conditions of stiffness can be treated only very approximately (see, e.g., Ref. [7] or Ref. [13]). Furthermore, it becomes even more difficult to compute polymer chain properties when the chain itself is confined to some space in many of the other methods. Although in this paper we do not calculate end-to-end distributions for the chains, we have shown, nevertheless, how to derive useful information about the constrained, stiff polymer.

We have demonstrated how the method accommodates potentials with angular dependence in three different ways. For a stiff lattice polymer constrained between two parallel plates, we showed that the polymer orientation behaves as expected during confinement. The integral equations for this lattice model are tractable to advanced stages in the computation. For a spherical pore we demonstrated another method by means of which stiffness can be assigned to a polymer chain through overlapping of more complicated monomer elements. Indeed, the formalism is quite generally applicable to a variety of polymer problems with more than positional degrees of freedom. In subsequent work we shall develop this formalism for a path integral formulation to include the investigation of the effects of lateral interactions.

ACKNOWLEDGMENTS

H.L.F. acknowledges the financial support of NSF Grant No. DMR 9628224. K.K.M.N. acknowledges the financial support of the National Research Foundation of South Africa.

APPENDIX A: PERSISTENCE LENGTH BY MEANS OF TRANSFER MATRIX

Defining the orientation of the i th segment of chain given by Eq. (2.2) $\hat{r}_i \in \{\pm \hat{x}, \pm \hat{y}, \pm \hat{z}\}$, the transfer matrix takes the form

$$\langle \hat{r}_i | T | \hat{r}_{i+1} \rangle = \begin{pmatrix} 1 & b & a & a & a & a \\ b & 1 & a & a & a & a \\ a & a & 1 & b & a & a \\ a & a & b & 1 & a & a \\ a & a & a & a & 1 & b \\ a & a & a & a & b & 1 \end{pmatrix}. \quad (\text{A1})$$

A persistence length for this model could then be computed by taking the average of $\hat{x}_1 \cdot \hat{x}_N$ by usual transfer matrix techniques. If one wishes to determine the persistence length when the chain is confined to two dimensions between the plates, the matrix above needs only to be reduced dimensionally.

APPENDIX B: GENERATING FUNCTIONS FROM Ξ

The monomer ensemble method introduced in Sec. I is completely general for the form of the fugacity term $z(\mathbf{r})$. Modification of z enables the use of the calculations for Ξ as a generating function.

If $z(\mathbf{r})$ were changed by the use of a parameter μ and an arbitrary three-dimensional vector ℓ in addition to the usual spatial constraint $z_{\text{constr}}(\mathbf{r})$ as follows:

$$z(\mathbf{r}) = z_{\text{constr}}(\mathbf{r}) e^{i\mu} e^{\mathbf{n} \cdot \ell}, \quad (\text{B1})$$

where \mathbf{n} is the segment orientation, this would result in $\Xi = \Xi(\mu, \ell)$ as given by Eq. (1.8).

Derivatives of Ξ with respect to ℓ then generate expressions in terms of $\sum_{\text{segments}} \mathbf{n} = \mathbf{R}_{\text{end-to-end}}$, i.e., the end-to-end distance of the chain. Suitable integration over μ would transform to canonical values.

In order to apply such a method the equations for ψ and $\hat{\psi}$ (1.6a), (1.6b) would then have to be solved for the new z . This would result in more complicated expressions than presented in the body of this paper and has been left for future work.

APPENDIX C: LATTICE BOUNDARY CONDITION AND CENTRAL VALUE EQUATIONS

Here we employ Eq. (2.4b) for different values of r_z and σ near the boundaries.

(1) For $r_z = r_z^0 + 1$, and for $\sigma = \uparrow, \downarrow$, and \parallel , respectively,

$$1 = \psi_{\uparrow}(r_z^0 + 1), \quad (\text{C1a})$$

$$1 = -z_0 \psi_{\downarrow}(r_z^0) + \psi_{\downarrow}(r_z^0 + 1), \quad (\text{C1b})$$

$$1 = \psi_{\parallel}(r_z^0 + 1). \quad (\text{C1c})$$

(2) For $r_z = r_z^0 + \frac{1}{2}$, and for $\sigma = \uparrow, \downarrow$, and \parallel , respectively,

$$1 = \psi_{\uparrow}\left(r_z^0 + \frac{1}{2}\right), \quad (\text{C2a})$$

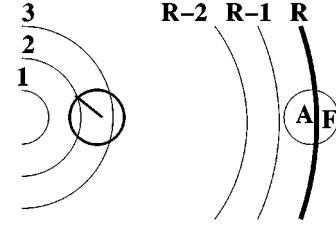


FIG. 5. Schematic representation of the integration procedure over shells. The shell numbering is illustrated, as well as the mixing between different shells. “F” represents the forbidden region for any bond of the polymer.

$$1 = -4az_0 \psi_{\parallel}(r_z^0) - z_0 \psi_{\downarrow}\left(r_z^0 - \frac{1}{2}\right) + \psi_{\downarrow}\left(r_z^0 + \frac{1}{2}\right), \quad (\text{C2b})$$

$$1 = -az_0 \psi_{\downarrow}(r_z^0) + \psi_{\parallel}\left(r_z^0 + \frac{1}{2}\right). \quad (\text{C2c})$$

(3) For $r_z = r_z^0$, and for $\sigma = \uparrow, \downarrow$, and \parallel , respectively,

$$1 = -bz_0 \psi_{\downarrow}(r_z^0) + \psi_{\uparrow}(r_z^0), \quad (\text{C3a})$$

$$1 = -4az_0 \psi_{\parallel}\left(r_z^0 - \frac{1}{2}\right) - z_0 \psi_{\downarrow}(r_z^0 - 1) + \psi_{\downarrow}(r_z^0), \quad (\text{C3b})$$

$$1 = -az_0 \psi_{\downarrow}\left(r_z^0 - \frac{1}{2}\right) + [1 - z_0(1 + 2a + b)] \psi_{\parallel}(r_z^0). \quad (\text{C3c})$$

(4) For $r_z = r_z^0 - \frac{1}{2}$, and for $\sigma = \uparrow$, and \parallel , respectively,

$$1 = -4az_0 \psi_{\parallel}(r_z^0) - bz_0 \psi_{\downarrow}\left(r_z^0 - \frac{1}{2}\right) + \psi_{\uparrow}\left(r_z^0 - \frac{1}{2}\right), \quad (\text{C4a})$$

$$1 = [1 - z_0(1 + 2a + b)] \psi_{\parallel}\left(r_z^0 - \frac{1}{2}\right) - az_0 \psi_{\downarrow}(r_z^0 - 1). \quad (\text{C4b})$$

(5) For $r_z = r_z^0 - 1$ and $\sigma = \uparrow$,

$$1 = -4az_0 \psi_{\parallel}\left(r_z^0 - \frac{1}{2}\right) - bz_0 \psi_{\downarrow}(r_z^0 - 1) + \psi_{\uparrow}(r_z^0 - 1). \quad (\text{C5})$$

Halfway between the plates the symmetry dictates that

$$\psi_{\uparrow,0} = \psi_{\downarrow,0}. \quad (\text{C6})$$

APPENDIX D: NUMERICAL INTEGRATION SCHEME FOR SPHERE-CONSTRAINED WALK

In order to elucidate the integration scheme used for the numerical calculations we refer to Fig. 5. The spherical geometry of the system is shown here up to the edge of the system. For each shell of thickness 1 we calculate $\psi_i = \phi_i^{(1)}$

$+n_z\phi_i^{(2)}$. Since the shells have the thickness of the radius of the bond, at each stage there are contributions from the two adjoining shells, according to Eq. (3.8). These can be summed if we assume that the values of $\phi_i^{(1)}$ and $\phi_i^{(2)}$ are constant and approximately equal to the value of the ϕ 's in

the *middle* of each shell. In the final shell ending at the radius R , the bond vector is permitted to move only in the allowed region A with zero weight in the forbidden region F of Fig. 5. The set $[\phi_i^{(1)}, \phi_i^{(2)}]$ is iterated through Eq. (3.8) until the values no longer change.

-
- [1] H. L. Frisch and J. -K. Percus, Phys. Rev. E **64**, 011805 (2001).
[2] H. L. Frisch and J. K. Percus, J. Phys. Chem. B **105**, 11834 (2001).
[3] K. Kroy and E. Frey, Phys. Rev. Lett. **77**, 306 (1996).
[4] J. Wilhelm and E. Frey, Phys. Rev. Lett. **77**, 2581 (1996).
[5] S. M. Aharoni and S. F. Edwards, Macromolecules **22**, 3361 (1989).
[6] K. K. Müller-Nedebock, S. M. Aharoni, and S. F. Edwards, Macromol. Symp. **98**, 701 (1995).
[7] T. B. Liverpool, R. Golestanian, and K. Kremer, Phys. Rev. Lett. **80**, 405 (1998).
[8] R. Golestanian and T. B. Liverpool, Phys. Rev. E **62**, 5488 (2000).
[9] P. J. Flory, *Statistical Mechanics of Chain Molecules* (Wiley Interscience, New York, 1969).
[10] F. F. Ternovsky, E. A. Zheltingovskaya, and A. R. Khokhlov, Makromol. Chem., Theory Simul. **2**, 151 (1993).
[11] S. Stepanow, J. Chem. Phys. **115**, 1565 (2001).
[12] B. Y. Ha and D. Thirumalai, J. Chem. Phys. **103**, 9408 (1995).
[13] B. Ha and D. Thirumalai, J. Chem. Phys. **106**, 4243 (1997).
[14] G. S. Chirikjian and Y. Wang, Phys. Rev. E **62**, 880 (2000).
[15] C. E. Cordeiro, M. Molisana, and D. Thirumalai, J. Phys. II **7**, 433 (1997).
[16] T. Pfohl *et al.*, Langmuir **17**, 5343 (2001).
[17] A. Gupta and S. Edwards, J. Chem. Phys. **98**, 1588 (1993).
[18] *Higher Transcendental Functions*, edited by A. Erdélyi (McGraw-Hill, New York, 1953), Vol. II.